

DOI:10.1002/ejic.201301407

Superhydrophobic Polyoxometalate/Calixarene Inorganic–Organic Hybrid Materials with Highly Efficient Desulfurization Ability

Xu-Miao Zhou,^{[a]†} Wei Chen,^{[a]†} and Yu-Fei Song^{*[a]}

Keywords: Polyoxometalates / Calixarenes / Hydrophobicity / Organic–inorganic hybrid composites

In this paper, imidazole-based ionic liquids with different alkyl chains were covalently grafted onto calix[4]arene, which resulted in the formation of **4–6** with the molecular formula $[C_{44}H_{56}O_4 \cdot 2C_4H_6N_2(CH_2)_n] \cdot 2Br$ [$n = 5$ (**4**), $n = 8$ (**5**), $n = 12$ (**6**)]. Ion exchange of **4–6** with $Na_9EuW_{10}O_{36} \cdot 32H_2O$ (denoted EuW_{10}) led to the formation of new inorganic–organic hybrid materials **7–9** with a molecular composition of $[C_{44}H_{56}O_4 \cdot 2C_4H_6N_2(CH_2)_n]_{4.5} \cdot EuW_{10}O_{36} \cdot xH_2O$ [$n = 5$, $x = 10$ (**7**); $n = 8$, $x = 7$ (**8**); $n = 12$, $x = 20$ (**9**)]. Contact angles above

139° suggested superhydrophobicity of the resulting hybrid materials **7–9**. Sulfur removal of dibenzothiophene by applying hybrid materials **7–9** as heterogeneous catalytic systems indicated that deep desulfurization could be achieved at $70^\circ C$ in 7, 5.5, and 5 min, respectively. Hybrid materials **7–9** were demonstrated to be highly efficient and selective desulfurization systems that could be reused more than 10 times without a clear decrease in reactivity.

Introduction

Calixarene is a macrocyclic receptor with phenol units linked to methylene groups at the *o,o'*-positions.^[1] As the third generation of host compounds, in addition to well-known crown ethers and cyclodextrins, calixarene has been actively studied and utilized as a building block, as it shows advantages over other molecular systems, including the fact that it has a hydrophobic cavity and that it can be easily modified by adding organic groups at both the lower and upper rims.^[2]

Polyoxometalates (POMs) are a class of early transition metal oxides of V, Mo, W, Nb, and so on. POMs cover an enormous size range and show a diverse range of dynamic molecular structures, a number of unique physical and chemical properties, and a wide range of applications.^[3] POMs, as transferable building blocks, hold considerable promise for the controlled assembly of large nanostructures and framework materials.^[4] Among the large domains of POMs, lanthanide-containing POMs with unique 4f-shell electrons show great potential as functional materials. For example, EuW_{10} shows a sandwich structure and has demonstrated its application as a fluorescent and catalytic material.^[5]

In recent years, a number of POMs have shown great potential as catalytic oxidative desulfurization catalysts. Sulfur-containing compounds in transportation fuels such as gasoline and diesel oil can be converted into SO_x during combustion, which is not only responsible for the formation of smog, sour gases, and acid rain, but it also poisons noble metal catalysts that can reduce SO_x emissions. The currently adopted method in industry is catalytic hydrodesulfurization (HDS).^[6] Although HDS is efficient in removing thiols, sulfides, and disulfides from fuels, it is less effective in removing refractory sulfur-containing compounds such as dibenzothiophene (DBT) and its derivatives.^[7] The harsh operating conditions and high capital cost of HDS largely restrict its application in the long run. Under such circumstances, deep desulfurization without the use of hydrogen, high pressures, and high temperatures is urgently needed. One desulfurization method that has been demonstrated to be potentially promising as an alternative to HDS is extractive catalytic oxidative desulfurization (ECODS), in which an ionic liquid (IL) is used as the extractant, H_2O_2 is used as the oxidant, and some efficient desulfurization catalysts such as POMs are used.^[8]

The combination of calixarene with metal–organic or inorganic clusters gives enormous structural diversity and leads to fascinating multifunctional assemblies owing to their inherently different natures and possible synergetic effects.^[9] For example, Konishi et al. reported the first porous organic–inorganic assemblies constructed from Keggin POM anions and calixarene– Na^+ complexes^[10] that display reversible guest sorption with retention of the original framework. In 2007, the same group reported interesting calix[4]arene-based hybrids that provide tunable hydro-

[a] State Key Laboratory of Chemical Resource Engineering, Beijing University of Chemical Technology, Beijing 100029, P. R. China
E-mail: songyufei@hotmail.com
songyf@mail.buct.edu.cn
<http://sci.buct.edu.cn/szll/jsml/wlhx/9778.htm>

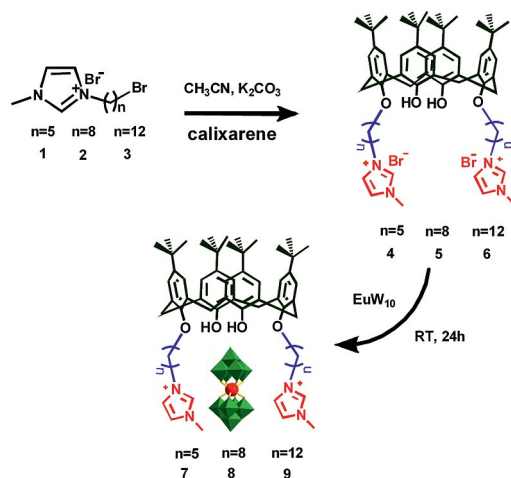
† These authors contributed equally to this work
Supporting information for this article is available on the WWW under <http://dx.doi.org/10.1002/ejic.201301407>.

phobic micropores for the facile recognition of the shape of simple alkanes and alkenes.^[11] Liao et al. reported a new hybrid based on the *p*-*tert*-butylthiacalix[4]arene-supported high-nuclearity inorganic cluster and Keggin POMs.^[12]

Inspired by the above contributions, herein, inorganic–organic hybrid materials **7–9** were synthesized by ion exchange of **4–6** [$C_{44}H_{56}O_4 \cdot 2C_4H_6N_2(CH_2)_n \cdot 2Br$] [denoted Calix-IL-Br, $n = 5$ (**4**), $n = 8$ (**5**), $n = 12$ (**6**)] with $Na_9EuW_{10}O_{36} \cdot 32H_2O$ (denoted EuW_{10}). The resulting hybrid materials exhibited superhydrophobicity and good extractive catalytic oxidative desulfurization ability under mild conditions.

Results and Discussion

As shown in Scheme 1, **4–6** with the molecular formula [$C_{44}H_{56}O_4 \cdot 2C_4H_6N_2(CH_2)_n \cdot 2Br$] [$n = 5$ (**4**), $n = 8$ (**5**), $n = 12$ (**6**)] denoted Calix-IL-Br were prepared by symmetric modification of the lower rim of calix[4]arene with ILs with different alkyl chains. Hybrid materials **7–9** were prepared by ion exchange of **4–6** with EuW_{10} , and they were characterized by FTIR and 1H NMR spectroscopy, thermogravimetric analysis (TGA), and contact-angle measurements.



Scheme 1. Schematic representation of the preparation process of inorganic–organic hybrid materials **7–9**.

As shown in Figure 1, the FTIR spectrum of EuW_{10} exhibits characteristic vibration bands of $W=O_d$, $W-O_b-W$, $W-O_c-W$, and $W-O_e-W$ at 945, 840, 779, and 696 cm^{-1} , respectively, in which O_d is the terminal oxygen atom, O_b is the bridge oxygen atom of two octahedrons sharing a corner, and O_c is the bridge oxygen atom of two octahedrons sharing an edge.^[13] In contrast, the FTIR spectrum of hybrid **7** displays the corresponding characteristic $W-O$ vibration signals at 940, 836, 780, and 713 cm^{-1} , respectively. The shifts are due to electrostatic interactions between the EuW_{10} anions and **4** in **7**. The FTIR spectra of **8** and **9** and their characteristic $W-O$ stretching bands are shown in Figure S1 (Supporting Information) and are summarized in Table 1.

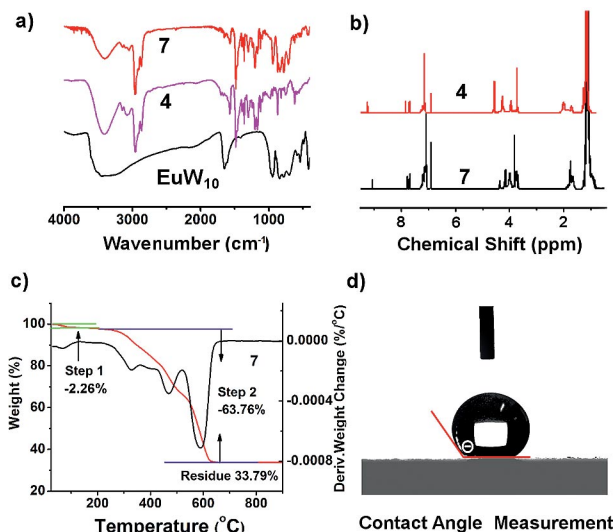


Figure 1. (a) FTIR spectra of EuW_{10} , **4**, and **7**. (b) 1H NMR spectra of **4** and **7**. (c) Thermogravimetric and differential thermal analysis of hybrid **7** with a scanning rate of 10 $^{\circ}C\ min^{-1}$. (d) Contact-angle measurement of hybrid **7**.

Table 1. FTIR $W-O$ stretching bands of EuW_{10} , **8**, and **9**.

Compound	Stretch [cm^{-1}]			
	$W=O_d$	$W-O_b-W$	$W-O_c-W$	$W-O_e-W$
EuW_{10}	945	840	779	696
8	935	836	781	710
9	940	837	776	714

The 1H NMR spectrum of **4** shows the signals of the $-OCH_2$, $-NCH_2$, and $-NCH_3$ groups at $\delta = 3.95$, 4.26, and 3.73 ppm, respectively, which are shifted to $\delta = 4.03$, 4.15, and 3.83 ppm, respectively, in hybrid **7**. Furthermore, the signals of the hydrogen atoms on the imidazole ring are shifted from $\delta = 7.69$, 7.85, and 9.23 ppm in **4** to $\delta = 7.67$, 7.76, and 9.07 ppm in **7**, respectively. Such shifts and signal broadening could be due to environmental changes resulting from electrostatic interactions between **4** and the EuW_{10} anions in **7**.

Similarly, the 1H NMR spectra of hybrids **8** and **9** (Figure S2, Supporting Information) and the assignment of the hydrogen atoms can be found in the Experimental Section, and they are in good agreement with the expected structures.

TGA of **7** was performed in air between 25 and 900 $^{\circ}C$ at a scanning rate of 10 $^{\circ}C\ min^{-1}$ (Figure 1c). A distinct multistep weight-loss process can be found in **7**. The first weight loss of 2.26% in the 25–140 $^{\circ}C$ range can be attributed to the loss of the crystallized water molecules. The weight loss of 63.76% in the 140–640 $^{\circ}C$ range is due to stepwise decomposition of the C–C, C–H, and C–N bonds through cleavage,^[14] which indeed include the decomposition of the alkyl chains, the calixarene, and the IL. Hybrids **8** and **9** also show multistep weight-loss processes (Figure S3, Supporting Information), which can be explained in a way similar to that of hybrid **7**.

The photoluminescent spectra of hybrids **7–9** in Figure 2 show five characteristic emission bands at 578 ($^5D_0 \rightarrow ^7F_0$), 594 ($^5D_0 \rightarrow ^7F_1$), 621 ($^5D_0 \rightarrow ^7F_2$), 653 ($^5D_0 \rightarrow ^7F_3$), 694 and 705 nm ($^5D_0 \rightarrow ^7F_4$), which correspond to the characteristic $^5D_0 \rightarrow ^7F_J$ ($J = 0, 1, 2, 3, 4$) transitions of Eu^{3+} .^[15,16]

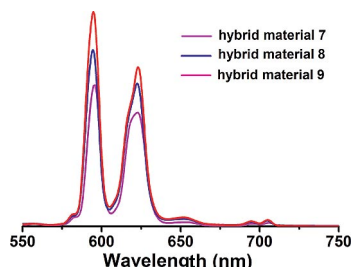


Figure 2. Fluorescence spectra of hybrids **7–9**.

To know the hydrophobicity of hybrids **7–9**, the contact angles were measured. The experimental results show a superhydrophobicity sequence of **9** (145.2°) > **8** (141.3°) > **7** (139.8°).^[17,18] Given that hybrids **7–9** show superhydrophobicity, this property is advantageous for the formation of hydrophobic/hydrophobic interactions and can be applied in the ECODS process, especially in the extraction process. This is because hydrophobic/hydrophobic interactions help substrates such as DBT to go into the interface, where the POM is oxidized by H_2O_2 to form an active peroxo species that can oxidize DBT to DBTO_2 . As a result, ECODS experiments with the use of **7–9** with H_2O_2 as oxidant were performed.^[19]

To investigate the effect of temperature on the desulfurization process, sulfur removal of DBT was performed at different temperatures (Figure 3). Taking **7** as an example, it shows 100% sulfur removal in 95, 35, 26, 15, and 7 min at 30, 40, 50, 60, and 70°C , respectively, in the presence of H_2O_2 . The oxidation product was demonstrated to be solely DBTO_2 (sulfone), which is indicative of the high efficiency and selectivity of **7**. In the case of **8** and **9**, deep desulfurization (100% sulfur removal) was achieved in 5.5 and 5 min, respectively, at 70°C .

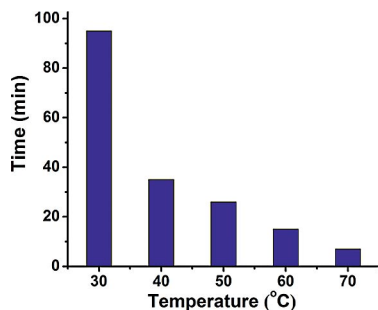


Figure 3. Times for 100% sulfur removal at different temperatures. Reaction conditions: H_2O_2 (0.048 mL); model oil (5 mL), sulfur content S = 1000 ppm; $\text{H}_2\text{O}_2/\text{DBT}/7 = 60:20:1$.

Notably, the addition of an IL is necessary to perform the desulfurization in all of the ECODS systems reported so far. In the current case, ILs with different alkyl chains were covalently tethered onto the calix[4]arene, and they

function as extractants for DBT; therefore, no extra IL was added in this particular case. Additionally, the experimental results show that the catalyst can be recycled at least 10 times with a slight decrease in the percentage of sulfur removed (100 to 95%). After each cycle, the catalyst was easily separated by filtration and washed with water and chloroform. Then, it was reused in a second round. The recycled catalyst was characterized by inductively coupled plasma (ICP) and FTIR and ^1H NMR spectroscopy (Figure S4, Supporting Information).

To disclose which component plays a role in the above desulfurization results, contrast experiments were performed, and the results are summarized in Table 2. Upon using calix[4]arene for desulfurization, less than 5% sulfur removal in 7 min was obtained (Table 2, Entry 1). Upon using $\text{H}_2\text{O}_2/\text{EuW}_{10}$ for desulfurization, almost no sulfur removal in the absence of an IL was observed (Table 2, Entry 2), which suggests that the oxidation does not take place without an IL. Upon using **1** and **4** (Table 2, Entries 3 and 4) for the desulfurization in the presence of H_2O_2 , 17.8 and 19.7% sulfur removal, respectively, was obtained at 70°C in 7 min. In contrast, deep desulfurization was achieved in 7 min by using hybrid **7** in the presence of H_2O_2 as the oxidant. Such a dramatic difference can be attributed to the combination of the superhydrophobicity and the catalytic desulfurization efficiency of hybrid **7**.

Table 2. Contrast experiments for the catalytic oxidative desulfurization of DBT at 70°C in 7 min.^[a]

Entry	Catalyst	$\text{H}_2\text{O}_2/\text{DBT}$	Sulfur removal (%)
1	calix[4]arene	3:1	<5
2	EuW_{10}	3:1	–
3	1	3:1	17.8
4	4	3:1	19.7
5	7	3:1	100

[a] Reaction conditions: H_2O_2 (0.048 mL); model oil (5 mL), sulfur content S = 1000 ppm; $\text{H}_2\text{O}_2/\text{DBT}/7 = 60:20:1$, 70°C .

Extension of the desulfurization time to 8 h did not help sulfur removal for calix[4]arene, EuW_{10} , and **1** alone. In the case of **4**, although IL moieties were covalently grafted onto the calix[4]arene, extension of the desulfurization time to 8 h caused only a slight increase in its ability to remove sulfur (19.7 to 27.3%). It can be concluded from the above contrast experiments that the synergistic effect of the calix[4]arene, the IL, and EuW_{10} play an important role in the highly efficient desulfurization result.

To obtain the kinetic parameters for the extractive catalytic oxidation desulfurization of DBT, experiments were performed with a molar ratio of $\text{H}_2\text{O}_2/\text{DBT}/7 = 60:20:1$ at 70°C . The percentage of sulfur removal and C_t are plotted against the reaction time in Figure 4, in which C_0 and C_t are the initial DBT concentration and the DBT concentration at time t , respectively. Linear fit of the data revealed that the catalytic reaction exhibits pseudo-zero-order kinetics for the desulfurization of DBT ($R^2 = 0.9931$). The rate constant k of the oxidation reaction was determined to be $173.29 \text{ ppm min}^{-1}$ on the basis of Equations (1) and (2). The

catalyst exhibits high catalytic efficiency for the oxidation of DBT to the corresponding sulfone with DBTO₂ as the only product.

$$\frac{-dC_t}{dt} = k \quad (1)$$

$$C_0 - C_t = kt \quad (2)$$

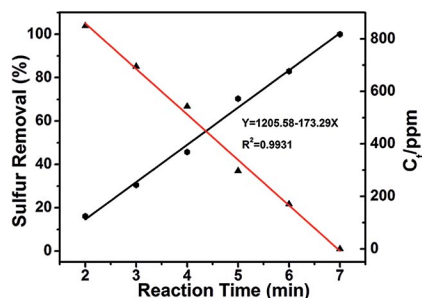


Figure 4. Sulfur removal of DBT and C_t as functions of the reaction time at 70 °C. $H_2O_2/DBT/7 = 60:20:1$.

To extend the applicability of inorganic–organic hybrid **7**, desulfurization of 4,6-DMDBT and BT (4,6-DMDBT = 4,6-dimethyldibenzothiophene; BT = benzothiophene) with **7** as the catalyst, H_2O_2 as the oxidant, and a molar ratio of H_2O_2 /substrate/**7** = 60:20:1 at 70 °C was performed. The experimental results showed 71.6 and 85.4% sulfur removal of BT and 4,6-DMDBT, respectively, at 70 °C in 30 min, and extension of the reaction time did not show a clear increase in the desulfurization efficiency. This reactivity of sulfur removal follows the order DBT > 4,6-DMDBT > BT, which is related to the electronic density of the S atoms and the steric hindrance of the substituent on the substrates. As is known, BT has the lowest electron density at the S atom, as well as the lowest reactivity, whereas the difference in electron density of 4,6-DMDBT and DBT is slight. Hence, the steric hindrance of the substrate plays a significant role in the different sulfur removal abilities of 4,6-DMDBT and DBT.

In the three-phase catalytic system (oil phase, interface, and solid phase), hydrophobic–hydrophobic interactions help substrates such as DBT to go into the interface, where EuW₁₀ is oxidized by H_2O_2 to form the active W–peroxo species that can oxidize DBT to DBTO₂.

Conclusions

To summarize, **4–6** were prepared by covalent tethering of imidazole-based ILs with different alkyl chains onto calix[4]arene. Ion exchange of **4–6** with EuW₁₀ led to the formation of hybrid materials **7–9**. The contact angles of **7–9** are >139°, which is indicative of the superhydrophobicity of the hybrid materials, and this is advantageous for the extraction of DBT through hydrophobic–hydrophobic interactions. As a result, extractive catalytic oxidative desulfurization (ECODS) by using **7–9** as catalysts in the presence of H_2O_2 as the oxidant is highly efficient and selective

for sulfur removal. Notably, if compared with other ECODS systems, the most important characteristic for **7–9** is that no extra addition of an IL is necessary. Moreover, the heterogeneous catalytic systems can be reused 10 times with only a slight decrease in reactivity. Therefore, inorganic–organic hybrids **7–9** are useful heterogeneous catalytic systems for deep desulfurization.

Experimental Section

Chemical Materials: All chemicals were purchased from AlfaAesar and were used without further purification. Acetone was distilled from potassium permanganate. Diethyl ether was distilled from sodium and benzophenone. Acetonitrile and chloroform were distilled from calcium hydride. All reactions were performed under nitrogen with dry solvents.

Measurements: ¹H NMR spectra were recorded with a Bruker AV 400 NMR spectrometer at a resonance frequency of 400 MHz, and the chemical shifts are given related to tetramethylsilane as an internal reference. FTIR spectra were recorded with a Bruker Vector 22 infrared spectrometer by using the KBr pellet method. Mass spectra were recorded with a Xevo G2 QT ESI mass spectrometer. C, H, and N elemental analyses were performed with a Vario EL cube from Elementar Analysis Systems. Thermogravimetric (TG) and differential thermal analysis (DTA) were performed with a TGA/DSC 1/1100 SF instrument from Mettler Toledo under N₂ with a heating rate of 10 °C min^{−1}. Fluorescence spectra were recorded with a Cary Eclipse fluorescence analyzer.

Synthesis: *p*-tert-Butylcalix[4]arene,^[20] 1-(5-bromopentyl)-3-methylimidazolium bromide (**1**), 1-(8-bromooctyl)-3-methylimidazolium bromide (**2**), and 1-(12-bromododecyl)-3-methylimidazolium bromide (**3**) were prepared and characterized according to literature methods.^[21] Compounds **4**, **5**, and **6** were synthesized by using a similar procedure, except for the use of ILs with different lengths of alkyl chains. The synthetic procedure for **4** is given as an example.

5,11,17,23-Tetra-tert-butyl-25,27-dihydroxy-26,28-bis(3-methylimidazol-1-ium-1-ylpentyl)calix[4]arene Bromide (4): To a solution of *p*-tert-butylcalix[4]arene (4.95 g, 7.6 mmol) in freshly distilled acetone (60 mL) was added 1-(5-bromopentyl)-3-methylimidazolium bromide (**1**; 4.75 g, 15.3 mmol) and K₂CO₃ (1.5 g, 10.8 mmol), and the reaction mixture was heated at reflux under N₂ for 6 d.^[22] After cooling the reaction mixture to room temperature, the solution was concentrated under vacuum. A bright yellow liquid was obtained as product **4**. Yield: 6.77 g (80.2%). ¹H NMR (400 MHz, [D₆]DMSO): δ = 1.13 [s, 18 H, -(CH₃)₃], 1.19 [s, 18 H, -(C(CH₃)₃)], 1.72 (m, 4 H, -CH₂-), 2.01 (m, 8 H, -CH₂-CH₂-), 3.73 (s, 6 H, -NCH₃), 3.95 (t, 4 H, -OCH₂-), 4.26 (t, 4 H, -NCH₂-), 4.56 (d, 8 H, Ar-CH₂-Ar), 6.90 (s, 2 H, Ar-OH), 7.14 (s, 8 H, ArH), 7.69 (s, 2 H, -CH₃NCHCHNC-), 7.85 (s, 2 H, -CNCHCHNCH₃), 9.23 (s, 2 H, -NCHNCH₃) ppm. IR (KBr): ν̄ = 3364 (s), 2964 (s), 2870 (m), 1572 (m), 1485 (s), 1362 (m), 1302 (m), 1202 (m), 1003 (m), 950 (w), 912 (w), 875 (m), 818 (w), 756 (w), 619 (m), 535 (w) cm^{−1}. MS: *m/z* = 1191 [M + Br][−].

5,11,17,23-Tetra-tert-butyl-25,27-dihydroxy-26,28-bis(3-methylimidazol-1-ium-1-ylloctyl)calix[4]arene Bromide (5): Yield: 81%. ¹H NMR (400 MHz, [D₆]DMSO): δ = 1.13 [s, 18 H, -(CH₃)₃], 1.18 [s, 18 H, -(C(CH₃)₃)], 1.42 [m, 16 H, -(CH₂)₄-], 1.80 [m, 8 H, -(CH₂)₂-], 3.86 (s, 6 H, -NCH₃), 3.94 (t, 4 H, -OCH₂-), 4.15 (t, 4 H, -NCH₂-), 4.17 (d, 8 H, -ArCH₂Ar-), 7.14 (s, 8 H, ArH), 7.71 (s, 2 H, -CH₃NCHCHNC-), 7.77 (s, 2 H, -CNCHCHNCH₃), 9.17 (s,

2 H, -NCHNCH₃) ppm. IR (KBr): $\tilde{\nu}$ = 3405 (s), 2953 (s), 2863 (m), 1571 (m), 1486 (s), 1456 (w), 1362 (m), 1299 (m), 1198 (s), 1170 (m), 1124 (m), 1023 (w), 871 (m), 755 (w), 622 (m) cm⁻¹. MS: m/z = 517 [M – 2 Br]²⁺.

5,11,17,23-Tetra-*tert*-butyl-25,27-dihydroxy-26,28-bis(3-methylimidazol-1-ium-1-yl)dodecyl)calix[4]arene Bromide (6): Yield: 72.7%. ¹H NMR (400 MHz, [D₆]DMSO): δ = 1.13 [s, 18 H, -C(CH₃)₃], 1.18 [s, 18 H, -C(CH₃)₃], 1.26 [s, 28 H, -(CH₂)₇-], 1.78 [m, 8 H, -(CH₂)₂-], 1.90 (m, 4 H, -CH₂-), 3.85 (s, 6 H, -NCH₃), 3.93 (t, 4 H, -OCH₂-), 4.15 (t, 4 H, -NCH₂-), 4.17 (d, 8 H, -ArCH₂Ar-), 7.13 (s, 8 H, -ArH), 7.72 (s, 2 H, -CH₃NCHCHNC-), 7.78 (s, 2 H, -CH₃NCHCHNC-), 9.15 (s, 2 H, -NCHNCH₃) ppm. IR (KBr): $\tilde{\nu}$ = 3420 (s), 2925 (s), 2854 (s), 1682 (w), 1560 (m), 1486 (s), 1362 (m), 1302 (m), 1199 (s), 1171 (m), 1124 (m), 1013 (w), 871 (m), 752 (w), 621 (m) cm⁻¹. MS: m/z = 573 [M – 2 Br]²⁺.

Synthesis of Hybrid Materials: Hybrids 7–9 were prepared by ion exchange of EuW₁₀ with 4–6, respectively. Compounds 4–6 were dissolved in distilled acetonitrile, and EuW₁₀ was dissolved in water. The two solutions were mixed, stirred at room temperature for 24 h, and then washed with water to obtain 7–9.

5,11,17,23-Tetra-*tert*-butyl-25,27-dihydroxy-26,28-bis(3-methylimidazol-1-ium-1-yl)pentyl)calix[4]arene–EuW₁₀ (7): ¹H NMR (400 MHz, [D₆]DMSO): δ = 1.11 [s, 18 H, -C(CH₃)₃], 1.17 [s, 18 H, -C(CH₃)₃], 1.77 (m, 12 H, -CH₂-), 3.83 (s, 6 H, -NCH₃), 4.03 (t, 4 H, -OCH₂-), 4.15 (t, 4 H, -NCH₂-), 4.24 (d, 8 H, Ar-CH₂-Ar), 7.09 (s, 8 H, ArH), 7.67 (s, 2 H, -CH₃NCHCHNC-), 7.76 (s, 2 H, -CNCHCHNCH₃), 9.07 (s, 2 H, -NCHNCH₃) ppm. IR (KBr): $\tilde{\nu}$ = 3408 (s), 2956 (s), 2864 (m), 1572 (m), 1485 (s), 1362 (m), 1301 (w), 1202 (m), 943 (s), 839 (w), 780 (s), 710 (m), 623 (w), 584 (w), 549 (w) cm⁻¹. (C₆₂H₈₆N₄O₄)_{4.5}EuW₁₀O₃₆·10H₂O (7026.35): calcd. C 47.65, H 5.79, N 3.59; found C 47.78, H 5.97, N 3.88. ICP: calcd. Eu 2.16, W 26.17; found Eu 2.22, W 26.56 (EuW₁₀, 36.55%).

5,11,17,23-Tetra-*tert*-butyl-25,27-dihydroxy-26,28-bis(3-methylimidazol-1-ium-1-yl)octyl)calix[4]arene–EuW₁₀ (8): ¹H NMR (400 MHz, [D₆]DMSO): δ = 1.14 [s, 18 H, -C(CH₃)₃], 1.18 [s, 18 H, -C(CH₃)₃], 1.61 [m, 16 H, -(CH₂)₄-], 1.77 [m, 8 H, -(CH₂)₂-], 3.81 (s, 6 H, -NCH₃), 3.96 (t, 4 H, -OCH₂-), 4.12 (t, 4 H, -NCH₂-), 4.15 (d, 8 H, -ArCH₂Ar-), 7.14 (s, 8 H, ArH), 7.68 (s, 2 H, -CH₃NCHCHNC-), 7.75 (s, 2 H, -CNCHCHNCH₃), 9.02 (s, 2 H, NCHNCH₃) ppm. FTIR (KBr): $\tilde{\nu}$ = 3387 (s), 2953 (s), 2867 (m), 1570 (w), 1485 (s), 1301 (w), 1200 (m), 1202 (m), 1167 (w), 1124 (w), 935 (s), 836 (m), 781 (m), 710 (m), 626 (w) cm⁻¹. (C₆₈H₉₈N₄O₄)_{4.5}EuW₁₀O₃₆·7H₂O (7350.74): calcd. C 49.95, H 6.19, N 3.43; found C 50.34, H 6.38, N 3.75. ICP: calcd. Eu 2.07, W 25.01; found Eu 2.10, W 25.45 (EuW₁₀, 34.94%).

5,11,17,23-Tetra-*tert*-butyl-25,27-dihydroxy-26,28-bis(3-methylimidazol-1-ium-1-yl)dodecyl)calix[4]arene–EuW₁₀ (9): ¹H NMR (400 MHz, [D₆]DMSO): δ = 1.13 [s, 18 H, -C(CH₃)₃], 1.18 [s, 18 H, -C(CH₃)₃], 1.26 [s, 28 H, -(CH₂)₇-], 1.77 [m, 8 H, -(CH₂)₂-], 3.61 (t, 4 H, -OCH₂-), 3.83 (s, 6 H, -NCH₃), 3.94 (t, 4 H, -NCH₂-), 4.36 (d, 8 H, Ar-CH₂-Ar), 7.13 (s, 8 H, -ArH), 7.70 (s, 2 H, -CH₃NCHCHNC-), 7.74 (s, 2 H, -CH₃NCHCHNC-), 9.12 (s, 2 H, -NCHNCH₃) ppm. IR (KBr): $\tilde{\nu}$ = 3424 (s), 2926 (s), 2854 (m), 1653 (m), 1557 (w), 1486 (s), 1384 (s), 1362 (m), 1299 (w), 1201 (m), 940 (m), 837 (m), 776 (s), 714 (m), 627 (w) cm⁻¹. (C₇₆H₁₁₄N₄O₄)_{4.5}EuW₁₀O₃₆·20H₂O (8089.44): calcd. C 50.73, H 6.84, N 3.12; found C 51.19, H 6.43, N 3.38. ICP: calcd. Eu 1.88, W 22.73; found Eu 1.96, W 23.17 (EuW₁₀, 31.75%).

Desulfurization Procedure and Analysis of S Content: A solution of DBT in *n*-octane was used as a model oil with a sulfur content S of 1000 ppm. The ECODS experiment was performed in a 50 mL

two-necked flask, to which 30 wt.-% H₂O₂ (0.048 mL, 0.47 mmol), model oil (5 mL, 0.157 mmol), and 7 (54.8 mg, 0.0078 mmol; 57.3 mg for 8, 63.1 mg for 9) were added. The resulting H₂O₂/DBT/EuW₁₀ molar ratio was 60:20:1. The reaction mixture was stirred at 30, 40, 50, 60, or 70 °C. During the reaction, samples of the upper layer of the model oil phase were periodically withdrawn and analyzed by GC with a flame ionization detector (GC–FID); DBT was identified by using reference standards. The content of DBT was analyzed with an Agilent 7820A GC system with a 30 m 5% phenylmethyl silicone capillary column with an inner diameter of 0.32 mm and 0.25 mm coating (HP-5). The analytical conditions were as follows: injection port temperature 340 °C, detector temperature 250 °C, oven temperature 70 °C, carrier gas ultrapure nitrogen, sample injection volume 1 μ L.

Supporting Information (see footnote on the first page of this article): FT-IR and ¹H NMR spectra for 7–9, TG-DTA curves for 8, 9.

Acknowledgments

This research was supported by the National Natural Science Foundation of China (21222104, 21076020), the Beijing Nova Program (2009B12), and the Fundamental Research Funds for the Central Universities (ZZ1227).

- [1] a) N. Morohashi, F. Narumi, N. Iki, T. Hattori, S. Miyano, *Chem. Rev.* **2006**, *106*, 529–5316; b) A. F. Danil de Namor, R. M. Cleverley, M. L. Z-Ormachea, *Chem. Rev.* **1998**, *98*, 2495–2525; c) J. S. Kim, D. T. Quang, *Chem. Rev.* **2007**, *107*, 3780–3799; d) A. Dondoni, A. Marra, *Chem. Rev.* **2010**, *110*, 4949–4977.
- [2] a) R. Joseph, C. P. Rao, *Chem. Rev.* **2011**, *111*, 4658–4702; b) A. Ikeda, S. Shinkai, *Chem. Rev.* **1997**, *97*, 1713–1734; c) D. M. Homden, C. Redshaw, *Chem. Rev.* **2008**, *108*, 5086–5130.
- [3] a) M. T. Pope, A. Müller, *Angew. Chem.* **1991**, *103*, 56–70; *Angew. Chem. Int. Ed. Engl.* **1991**, *30*, 34–48; b) C. L. Hill, *Chem. Rev.* **1998**, *98*, 1–2; c) L. Cronin, A. Müller, *Chem. Soc. Rev.* **2012**, *41*, 7333–7334; d) D.-L. Long, L. Cronin, *Dalton Trans.* **2012**, *41*, 9815–9816; e) E. Coronado, C. Giménez-Saiz, C. J. Gómez-García, *Coord. Chem. Rev.* **2005**, *249*, 1776–1796; f) Y. F. Song, R. Tsunashima, *Chem. Soc. Rev.* **2012**, *41*, 7384–7402; g) D.-Y. Du, L.-K. Yan, Z.-M. Su, S.-L. Li, Y.-Q. Lan, E.-B. Wang, *Coord. Chem. Rev.* **2013**, *257*, 702–717; h) A. Proust, B. Matt, R. Villanneau, G. Guillemot, P. Gouzerh, G. Izzet, *Chem. Soc. Rev.* **2012**, *41*, 7605–7622; i) Y.-F. Song, D.-L. Long, L. Cronin, *Chem. Rev.* **2011**, *11*, 158–171.
- [4] a) Y.-F. Song, N. McMillan, D.-L. Long, J. Thiel, Y. L. Ding, H.-S. Chen, N. Gadegaard, L. Cronin, *Chem. Eur. J.* **2008**, *14*, 2349–2354; b) Y. P. Jeannin, *Chem. Rev.* **1998**, *98*, 51–76; c) A. Corma, F. X. Xamena, *Chem. Rev.* **2010**, *110*, 4606–4655; d) N. Stock, S. Biswas, *Chem. Rev.* **2012**, *112*, 933–969; e) S. Zhao, L. Huang, Y.-F. Song, *Eur. J. Inorg. Chem.* **2013**, 1659–1663.
- [5] a) Z.-L. Wang, R. Zhang, Y. Ma, A. Peng, H. Fu, J. Yao, *J. Mater. Chem.* **2010**, *20*, 271–277; b) J. Xu, S. Zhao, W. Chen, M. Wang, Y.-F. Song, *Chem. Eur. J.* **2012**, *18*, 4775–4781; c) M. Jiang, X. Zhai, M. Liu, *Langmuir* **2005**, *21*, 11128–11135; d) K. Binnemans, *Chem. Rev.* **2007**, *107*, 2592–2614; e) Z. Han, Y. Guo, R. Tsunashima, Y.-F. Song, *Eur. J. Inorg. Chem.* **2013**, 1475–1480; f) X. Wang, J. Wang, R. Tsunashima, K. Pan, B. Cao, Y.-F. Song, *Ind. Eng. Chem. Res.* **2013**, *52*, 2598–2603.
- [6] M. Francisco, A. Arce, A. Soto, *Fluid Phase Equilib.* **2010**, *294*, 39–48.
- [7] A. Rothlisberger, R. Prins, *J. Catal.* **2005**, *235*, 229–240.
- [8] a) W. Zhu, H. Li, X. Jiang, Y. Yan, J. Lu, L. He, J. Xia, *Green Chem.* **2008**, *10*, 641–646; b) H. Li, W. Zhu, Y. Wang, J. Zhang, J. Lu, Y. Yan, *Green Chem.* **2009**, *11*, 810–815; c) J. Zhang, W.

- Zhu, H. Li, W. Jiang, Y. Jiang, W. Huang, Y. Yan, *Green Chem.* **2009**, *11*, 1801–1807; d) Y. Ding, W. Zhu, H. Li, W. Jiang, M. Zhang, Y. Duan, Y. Chang, *Green Chem.* **2011**, *13*, 1210–1216.
- [9] T. N. Ursales, I. Silaghi-Dumitrescu, R. Grecu, L. Silaghi-Dumitrescu, N. Popovici, E.-J. Popovici, *J. Optoelectron. Adv. Mater.* **2004**, *6*, 471–476.
- [10] Y. Ishii, Y. Takenaka, K. Konishi, *Angew. Chem.* **2004**, *116*, 2756–2759; *Angew. Chem. Int. Ed.* **2004**, *43*, 2702–2705.
- [11] Y. Ishii, N. Nakayama, K. Konishi, *Chem. Lett.* **2007**, *36*, 246–247.
- [12] Y. Bi, S. Du, W. Liao, *Chem. Commun.* **2011**, *47*, 4724–4726.
- [13] a) R. D. Peacock, T. J. R. Weakley, *J. Chem. Soc. A* **1971**, 1836–1839; b) M. Jiang, X. Zhai, M. Liu, *Langmuir* **2005**, *21*, 11128–11135; c) M. Jiang, M. H. Liu, *J. Colloid Interface Sci.* **2007**, *316*, 100–106.
- [14] a) Y.-F. Song, D.-L. Long, L. Cronin, *Angew. Chem.* **2007**, *119*, 3974–3978; *Angew. Chem. Int. Ed.* **2007**, *46*, 3900–3904; b) J. Xu, S. Zhao, Y. Ji, Y.-F. Song, *Chem. Eur. J.* **2013**, *19*, 709–715; c) Y.-F. Song, D.-L. Long, L. Cronin, *CrystEngComm* **2010**, *12*, 109–115.
- [15] X. Wang, J. Wang, R. Tsunashima, K. Pan, B. Cao, Y.-F. Song, *Ind. Eng. Chem. Res.* **2013**, *52*, 2598–2603.
- [16] a) G. Blasse, G. J. Dirksen, F. Zonnevijlle, *J. Inorg. Nucl. Chem.* **1981**, *43*, 2847–2854; b) M. J. Stillman, A. J. Thomson, *J. Chem. Soc., Dalton Trans.* **1976**, 1138–1144.
- [17] S. Varghese, A. K. Lele, D. Srinivas, R. A. Mashelkar, *J. Phys. Chem. B* **2001**, *105*, 5368–5373.
- [18] S. Wang, L. Feng, H. Liu, T. Sun, X. Zhang, L. Jiang, D. Zhu, *ChemPhysChem* **2005**, *6*, 1475–1478.
- [19] a) W. Huang, W. Zhu, H. Li, H. Shi, G. Zhu, H. Liu, G. Chen, *Ind. Eng. Chem. Res.* **2010**, *49*, 8998–9003; b) W. Zhu, H. Li, X. Jiang, Y. Yan, J. Lu, L. He, J. Xia, *Green Chem.* **2008**, *10*, 641–646; c) W. H. Lo, H. Y. Yang, G. T. Wei, *Green Chem.* **2003**, *5*, 639–642.
- [20] a) C. D. Gutsche, M. Iqbal, D. Stewart, *J. Org. Chem.* **1986**, *51*, 742–745; b) C. D. Gutsche, M. Iqbal, *Org. Synth.* **1993**, *8*, 75–77; c) C. D. Gutsche, B. Dhawan, K. H. No, R. Muthukrishnan, *J. Am. Chem. Soc.* **1981**, *103*, 3782–3792.
- [21] M.-B. Moity, A. Quadi, V. Mazan, S. Miroshnichenko, D. Ternova, S. Georg, M. Sypula, C. Gaillard, I. Billard, *Dalton Trans.* **2012**, *41*, 7526–7536.
- [22] Z.-T. Li, G.-Z. Ji, C.-X. Zhao, S.-D. Yuan, H. Ding, C. Huang, A.-L. Du, M. Wei, *J. Org. Chem.* **1999**, *64*, 3572–3584.

Received: November 3, 2013

Published Online: January 17, 2014